Korean J. Chem. Eng., **31**(7), 1174-1179 (2014)
DOI: 10.1007/s11814-014-0024-4

pISSN: 0256-1115
eISSN: 1975-7220

Hydrogenolysis of nitrosodimethyl amine in gas phase over Au/γ-Al_2O_3 nanocatalyst

Shahram Ghanbari Pakdehi[*,†] **and Fariba Fazeli**[**]

*Faculty Chemical Engineering, Malek Ashtar University of Technology, P. O. Box 11365-8486, Tehran, Iran
**Space Transportation Research Institute, Iranian Space Research Center, P. O. Box 13445-754, Tehran, Iran

(*Received 28 November 2013 • accepted 18 January 2014*)

Abstract−Nitrosodimethyl amine (NDMA), as a carcinogenic byproduct in production of unsymmetrical dimethyl hydrazine (UDMH) in space industries, should be decomposed in the vapor phase. A suitable method for this purpose is selective catalytic hydrogenolysis of NDMA over Au/γ-Al_2O_3 nanocatalyst. We synthesized and characterized the Au/γ-Al_2O_3 nanocatalyst by homogeneous deposition-precipitation (HDP)/DP-urea method. Activity of the catalyst was influenced by nanosized Au particles, Au loading and the bed temperature. The optimum parameters for the catalyst were: Au particles <5 nm, Au loading at 1.5 wt% and bed temperature of 35-45 °C. The reaction was strongly sensitive to the Au particle size. The reaction occurred over the catalyst to produce dimethyl amine (DMA) and nitroxyl in a selective manner. The kinetics of NDMA hydrogenolysis over the nanocatalyst was studied in an integral fixed bed reactor. There existed a consistency with the Langmuir-Hinshelwood mechanism involving dissociative adsorption of H_2 and NDMA.

Keywords: NDMA Hydrogenolysis, Au/γ-Al_2O_3 Nanocatalyst, Effective Parameters, Au Particle Size, Kinetics

INTRODUCTION

Unsymmetrical dimethyl hydrazine (UDMH) is used as a liquid fuel in space programs. It is the outcome of the reaction between dimethyl amine (DMA) and monochloroamine in aqueous phase [1]:

$$(CH_3)_2NH+NH_2Cl \rightarrow (CH_3)_2NNH_2+HCl \quad (1)$$

Due to this reaction, nitrosodimethyl amine (NDMA) is formed as a byproduct from the reaction between monochloramine and UDMH [1]:

$$NH_2Cl+(CH_3)_2NNH_2+0.5O_2 \rightarrow (CH_3)_2NNO+NH_4Cl \quad (2)$$

NDMA is a semi-volatile substance. There are low concentrations of NDMA in the air at the UDMH production plants [2]. This substance is a highly carcinogenic, mutagenic and teratogenic chemical. The esophagus and liver are the primary tumor formation sites for NDMA. Other organs such as the bladder, brain and lungs are the targets for this chemical as well [3]. Due to its high solubility in water, gas absorption is a conventional method for its removal from air [4]. However, destruction of absorbed DNMA in water is expensive [5-7]. A method for destruction of NDMA to less hazardous compound(s) is direct catalytic hydrogenolysis of NDMA vapors in a catalytic environment. Similar reactions have been reported by noble metal catalysts. Rh is the best catalyst for this purpose [8], but it is very expensive. Therefore, studies continue in an effort to find a catalyst with lower price and easier operating conditions (temperature, pressure, etc.). Because of the dangerous nature of hydrogen at high temperatures, it is desirable to conduct the reaction at low temperatures.

Haruta demonstrated that nanosized particles of gold impregnated on oxide supports possess a high catalytic activity for some reactions at low temperatures [9]. On the other hand, γ-Al_2O_3 has been used extensively as an oxide support for many monometallic catalysts used in hydrogenation reactions. Therefore, nanosized Au/γ-Al_2O_3 catalyst may destruct NDMA at low temperatures. Another advantage of gold catalyst is its low cost compared with the Pt catalysts for the last ten years. In general, there exists some information about using gold nanocatalysts in hydrogenation of nitro compounds [10-12], but there is no report for using gold nanocatalyst in NDMA hydrogenolysis in gas phase.

The objectives of this study are the synthesis and application of Au/γ-Al_2O_3 nanocatalyst in the catalytic hydrogenolysis of NDMA in gas phase. Effective parameters on the reaction are investigated in a flow reactor. Finally, a reaction mechanism is proposed, based on which a reaction rate model is derived.

EXPERIMENTAL

1. Chemical

The chemicals used in this study all were of the analytical grade. Chloroauric acid (Aldrich Co.), γ-Al_2O_3 with a 250 m^2g^{-1} surface area (Qingdao Wish Chemicals, China), NDMA (Aldrich Co.) and hydrogen gas (>99.99% purity, Roham Gas Co.) were all purchased.

2. Catalyst Synthesis

The Au/γ-Al_2O_3 nanocatalyst was synthesized by the homogeneous deposition-precipitation (HDP)/DP-urea method [9,12]. Urea (as the basification agent) was added to a solution of $HAuCl_4 \cdot 3H_2O$. Also, γ-Al_2O_3 (d_p=1 mm) was added to the solution. The resultant suspension was stirred up to 20 hours at 87 °C temperature. The pH of the suspension was increased progressively to reach ca.7 after 20 hours as a result of thermally-induced urea decomposition. The solid phase was separated by centrifugation, washed six times with deionized water and dried under the vacuum at room temperature

---

[†] To whom correspondence should be addressed.
E-mail: sh_ghanbari73@yahoo.com

overnight. At this stage, the catalyst was orange colored. It was reduced under H_2 gas from ambient temperature to 177 °C, then held constant for 7 hours at 177 °C. Finally, it was cooled down to the desired temperature. The color changed to pink purple (reduction of Au^{3+} to Au^{o}).

3. Catalyst Characterization

The Au content was determined (within ±2%) by ICP analysis system (model CE 7500, Agilent). The chlorine content was detected by XRF (model Philips-PW 1480) and measured by HPLC equipped with conductivity detector (model WATERS 600E).

BET surface areas were measured by nitrogen adsorption at −196 °C applying a Micromeritics ASAP 2010 apparatus. The XRD analysis of the catalyst particles was performed using a D/MAX 2500 powder X-ray diffractometer with Cu Ka radiation (c=0.154 nm). The 2 h angles were scanned from 5° to 80°.

The TEM studies were carried out using a high-resolution JEOL 2010 microscope (operated at 200 kV). Several bright field TEM images of different portions of the same samples were obtained at magnifications of up to 400000. At least 100 particles were counted to determine the average particle size. Average particle size of Au was calculated through $\bar{d}_p=\sum n_i d_i^3/\sum n_i d_i^2$ where, $\bar{d}_p$ is the average diameter of Au particles and n_i is the number of particles of diameter d_i.

4. Hydrogenolysis Experiments

The gas phase hydrogenolysis of NDMA was carried out in a fixed-bed continuous flow microreactor made of quartz (12 mm inner diameter and 70 mm length) using 1 g of the nanocatalyst. The reactor was placed in an electrical tube furnace and heated within ±2 °C accuracy range. The reaction temperature was monitored by a digital temperature controller (Omega) equipped with a J-type thermocouple installed at the center of the bed.

Before the experiments, all catalysts were reduced in situ in pure hydrogen flow from ambient temperature to 176 °C and kept constant for 2 hours at 176 °C. Finally, the nanocatalysts were cooled to certain temperatures under pure H_2 gas.

Liquid NDMA was poured into the tri-neck flask that was held in a water bath in a hanging manner. The NDMA vapor was fed into the reactor by bubbling hydrogen and nitrogen (as the diluent gas) mixture through liquid NDMA at nearly atmospheric pressure. The amount of reactant injected into the H_2 stream was determined by the ratio of the NDMA partial pressure (vapor pressure) to the total pressure. The feed mixture (NDMA+H_2+N_2) was introduced into the reactor with a space velocity of 30,000 $mL\cdot g^{-1}\cdot h^{-1}$ (GHSV=20,000 h^{-1}). The concentration of NDMA was controlled by either the nitrogen flow rate or water bath temperature.

The reaction was studied at various temperatures in 5 °C to 45 °C range. The catalyst activity was expressed in $mmol\cdot g_{catalyst}^{-1}\cdot s^{-1}$. The gases released from this reactor were collected and analyzed as an integral reactor to cover a wide range of conversions.

5. Analysis

The products were analyzed by an online gas chromatograph (HP 4890, equipped with TCD detector). The column temperature was 300 °C. Helium was used as carrier gas. For the reactants and products, the retention times and sensitivity factors were calibrated using several gas mixtures. The concentrations of the produced gases were measured. The experiment was stopped when the outlet concentrations reached the steady values.

RESULTS AND DISCUSSION

1. Catalyst Characterization

The XRD patterns of γ-Al_2O_3 and Au/γ-Al_2O_3 showed a good dispersion of gold particles within the γ-Al_2O_3 support [12]. The TEM image of the Au/γ-Al_2O_3 catalyst illustrated the catalyst particle size distribution between 1.8 and 7.8 nm with an average particle size of 4.8 nm. Nevertheless, the major part of these particles' size was between 3 and 6 nm [12]. Moreover, according to previous work of these authors, the amount of chlorine in the reduced catalyst was <0.1 ppm [12]. Presence of chlorine led to obtaining larger Au particle size in the same reduction conditions [13].

2. Effective Parameters On The Reaction Conversion

Preliminary experiments indicated that there was no reaction between NDMA and hydrogen vapors up to 150 °C. In the experiments using bulk gold metal as the reaction catalyst no reaction was observed, while in the presence of nanosized Au/γ-Al_2O_3 catalyst a reductive destruction of NDMA was observed. The effective parameters were evaluated by feeding at space velocity of 30,000 $mL\cdot g^{-1}\cdot h^{-1}$ (GHSV=20,000 h^{-1}). The results were reproducible with a mean absolute deviation of 3%.

In the presence of conventional transition metal catalysts (Pd, Pt etc.), the hydrogenation of NDMA produces UDMH [1]:

$$(CH_3)_2NNO+2H_2 \rightarrow (CH_3)_2NNH_2+H_2O \tag{3}$$

Experiments were conducted in the presence of Au/γ-Al_2O_3 nanocatalyst where the gas phase products were trapped in water. Analysis of gas and liquid phases [14-16] indicated that the products were dimethyl amine (DMA) and nitroxyl (HNO). The N-N bond in NDMA was cleaved and DMA with carbon balance in excess of 99% was produced. Moreover, the total mass balance of nitrogen in the reactor was 99±1%. The mass balance for N-containing products was 59.2% and 39.8±1% for DMA and HNO, respectively. No other nitrogen containing intermediates or products were detected, while reaction Eq. (4) occurred in the catalytic hydrogenolysis of NDMA:

$$(CH_3)_2NNO+H_2 \rightarrow (CH_3)_2NH+HNO \tag{4}$$

Here, DMA and HNO are non-carcinogen compared with NDMA.

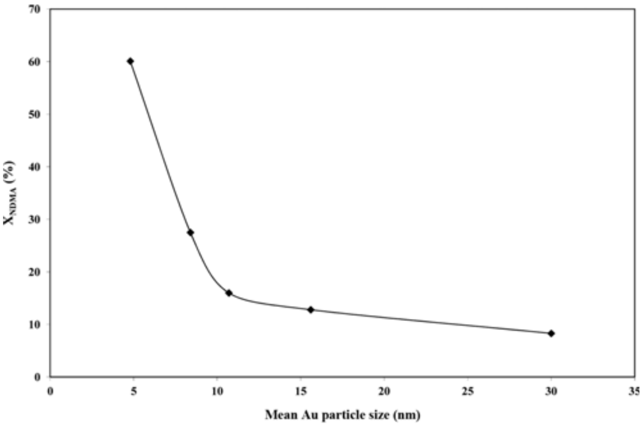

Fig. 1. Effect of Au particle size on the reaction conversion (Au loading=1.5 wt%, T=30 °C, $C_{o,NDMA}$=0.1 $mmol\cdot L^{-1}$, Q_F=50 $mL\cdot min^{-1}$).

3. Effect of Au Particle Size

If Au solution is added to γ-Al_2O_3 at various stirring times and addition rates or vice versa, different sizes of Au particles will be obtained. In other words, stirring times and addition rates will control the preparation of Au particles. Au particle size contributes to the reaction conversion (Fig. 1), where the higher conversions occurred in smaller size of Au particles due to more available surface area for Au as the reaction surface.

Although there is no explanation on the special activity of gold so far and the actual mechanism of the catalyzed reaction is not fully understood, the small Au nanoparticles (<5 nm) have the higher hydrogen uptake per surface atom. At this size, the surface consists of atoms at corner and edge positions. Thus, it was proposed that hydrogen atoms are only adsorbed and dissociated at edges and corners of the gold particles [9,17-19]. In other words, size reduction of Au particles leads to an increase in the concentration of low coordinated step, edge and kink sites. Since the electron orbitals' overlap decreases as the average number of bonds between the atoms decreases, the surface atoms become more reactive and begin to behave more as individual atoms [20].

4. The Au Loading Effect

Another parameter affecting the conversion of the reaction was Au loading (Fig. 2). As it is shown, an increase in Au loading up to 1.5 wt% led to an increase in the conversion; here the conversion follows a decreasing trend above 1.5 wt%. It is because of the tendency of Au particles to grow and form larger Au clusters within the pores. In a similar work, Comotti observed such a phenomenon [21]. It is observed that no reaction occurs in zero content Au, indicating that the hydrogenolysis of NDMA is only carried out on the gold nanoparticles and that the support does not participate directly in the reaction.

5. The Bed Temperature Effect

Among the environmental parameters on the reaction, bed temperature decrease revealed an interesting effect (Fig. 3). As it was stated, no hydrogenolysis reaction was observed for NDMA in the presence of bulk gold up to 150 °C. Using nanosized Au, the reaction occurred at low temperatures. In this case, it was completed at 40 °C and no appreciable reaction was observed below 7 °C as the temperature decreased.

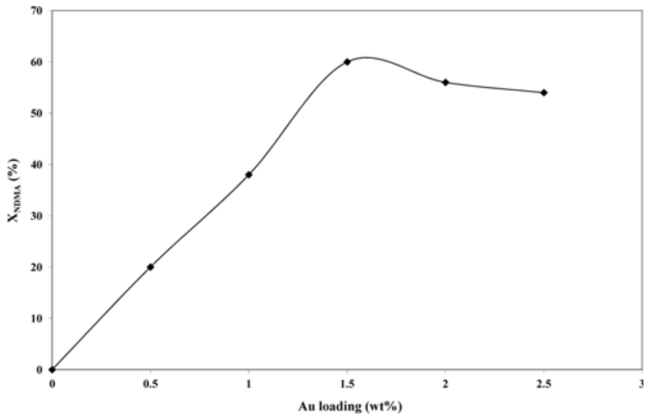

Fig. 2. Effect of Au loading on the reaction conversion (mean particle size of Au=4.8 nm, T=30 °C, $C_{o,NDMA}$=0.1 mmol·L^{-1}, Q_F= 50 mL·min^{-1}).

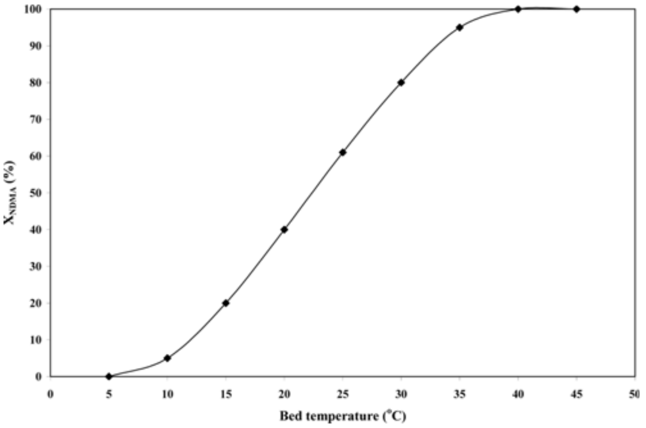

Fig. 3. Effect of bed temperature on the reaction conversion (mean particle size of Au=4.8 nm, Au loading=1.5 wt%, $C_{o,NDMA}$= 0.1 mmol·L^{-1}, Q_F=50 mL·min^{-1}).

6. Catalyst Deactivation

Heterogeneous catalytic reactions may generally be affected by deactivation for three reasons: 1) chlorine content in the prepared nanocatalyst, 2) irreversible change of the catalytic surface under reaction conditions (textural change or sintering) and 3) deposition of carbonaceous residues from reactants, products or intermediates as coking.

Similar works about hydrogenation reaction with Au/γ-Al_2O_3 nanocatalyst indicated that the chloride ion inhibited the reaction. It was important to control or eliminate the amount of chlorine which poisoned the gold nanocatalysts during preparation [13,22]. In this research, chlorine content was measured as <0.1 ppm. So, the first reason was not correct.

Hydrogenolysis of NDMA is exothermic ($\Delta H_{r,298\,K}$=−182.28 kJ/mol, computed from ASTM Program CHETAH 7.2), which may lead to an increase in bed temperature. As it will be observed, since the NDMA concentration was diluted by N_2, the temperature rise of the bed was not significant. Experimentally, the maximum temperature rise in the bed was observed as to be about 50 °C. In the next section, to prevent the hot zones in the catalyst bed, γ-Al_2O_3 (as inert solid diluents) would be added into the bed. On the other hand, most

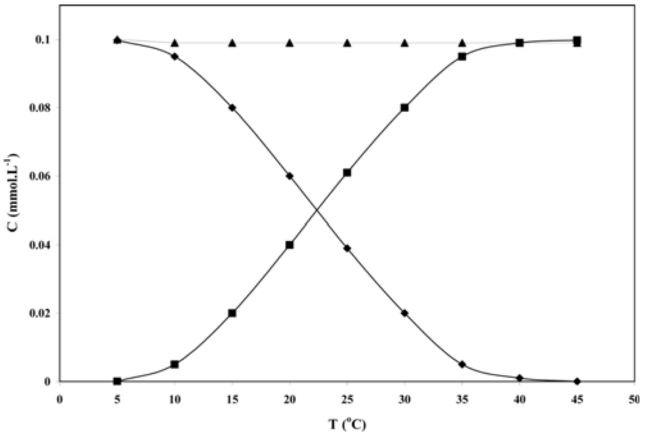

Fig. 4. Progress diagram of catalytic hydrogenolysis of NDMA over 1.5 wt% Au/γ-Al_2O_3, $C_{o,NDMA}$=0.1 mmol·L^{-1} (-◆- NDMA, -■- DMA, -▲- carbon balance).

reported works indicate that sintering of gold particles occurred above 200 °C [23]; hence it could be deduced that the nanocatalyst deactivation did not occur due to lack of sintering phenomenon.

In the temperature range from ambient up to 45 °C, there was a carbon balance between the initial feed (containing NDMA) and the final products (containing DMA and unreactead outlet NDMA). The destruction of NDMA and formation of DMA as a function of temperature over the Au/γ-Al_2O_3 nanocatalyst is shown in Fig. 4. The disappearance of the reactant corresponded to the formation of DMA; therefore, there was no deposition of carbonaceous residues. The third reason was not valid either. In other words, the nanocatalyst was not deactivated under the conditions applied.

7. Kinetic Study

1.5 wt% Au/γ-Al_2O_3 with 4.5 nm in Au size was found to be the most effective catalyst for destruction of NDMA in the vapor phase. So, all kinetic studies were carried out using 1 g of this catalyst. The reactor was operated and analyzed as an integral reactor, covering a wide range of conversions. Under all operating conditions, the overall errors in determining the mole-fraction of NDMA in the reactor effluent were less than ±3%.

Kinetic study was performed in a plug flow microreactor. To ensure a plug flow pattern in gas-solid system, the catalyst bed length (l) should be at least 50 particle diameters ($l/d_p>50$) [24]. This criterion was observed in this work ($l=7$ cm, $d_p=1$ mm, $l/d_p=70$).

Since the catalytic hydrogenolysis of NDMA is exothermic, it may lead to hot-spot or non-homogeneity of temperature in the reactor. To prevent this phenomenon, the experimental methods for reducing temperature gradients were mainly the dilution of both feed and catalyst and decreasing the reactor diameter. The feeding of an inert substance together with reactants allows increasing the heat removal from the reaction zone. The catalyst dilution through inert solid particles with the same size of the catalytic particles reduces the local hot-spot and improves the temperature distribution along the catalytic bed. A reduction in reactor diameter should necessarily be accompanied by the reduction of particle diameter, in order to fulfill the plug flow conditions. Generally, for plug flow conditions the inner reactor diameter (ID) must be higher than at least ten-times the catalyst particle diameter (d_p) ($ID/d_p>10$) [24]. In this study, the feed was diluted by N_2 inert gas. The bed was diluted by γ-Al_2O_3 particles (as inert support) with the same size of Au/γ-Al_2O_3 nanocatalyst particles. The reactor was vibrated gently for allowing the diluents to settle in the voids of the catalyst bed. The ID/d_p was selected as being 12.

For the kinetic study, the mass transfer resistances have to be excluded by proper adjustment of the appropriate reaction conditions in the reactor. In this case, interphase gradients (external diffusion) and intraphase gradients (internal diffusion) should be reduced [24]. To eliminate the influence of mass transfer between gas and solid on the reaction rate (interphase gradients), the effect of feed flow rate on the conversion of NDMA was studied in the same gas residence time duration. The conversion of reactant will change until the interphase limitations (external diffusion) appear (Fig. 5). As it is shown, the interphase gradients can be reduced by increasing the flow rate of reactants.

The influence of catalyst particle size on the reaction rate was studied to ensure the negligible effect of internal diffusion on the reaction rate [24]. For this purpose, 1.5 wt% Au/γ-Al_2O_3 catalysts with various particle diameters, between 0.5 mm and 2.4 mm, were synthesized and tested (Fig. 6). In this figure, the intraphase mass transfer limitations were minimized by a decrease in the pellet size of the catalyst.

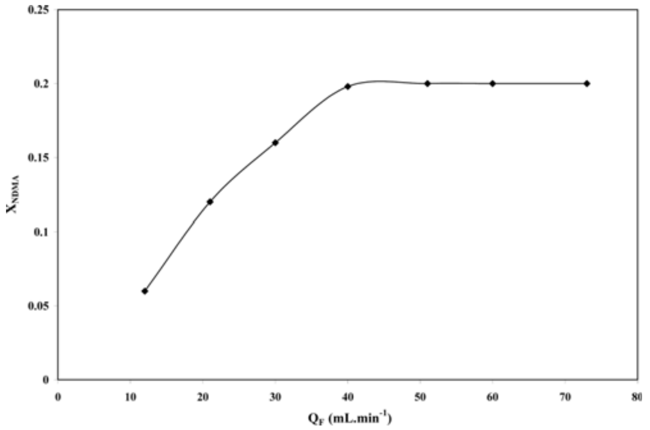

Fig. 5. Influence of flow rate on conversion at a constant space velocity for checking presence of interphase mass transfer limitations.

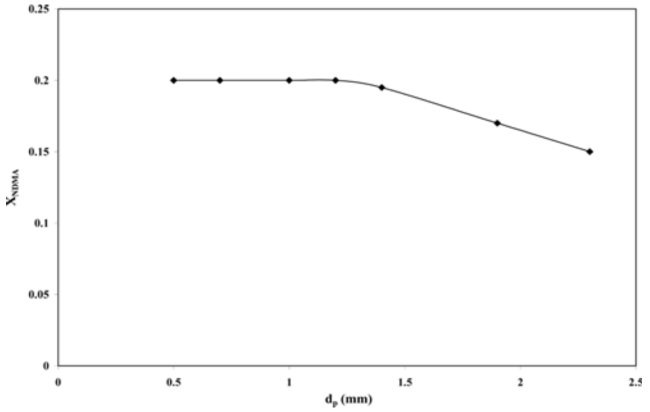

Fig. 6. Experimental test for influence of catalyst particle diameter (d_p) on the conversion to evaluate intraphase mass transfer limitations.

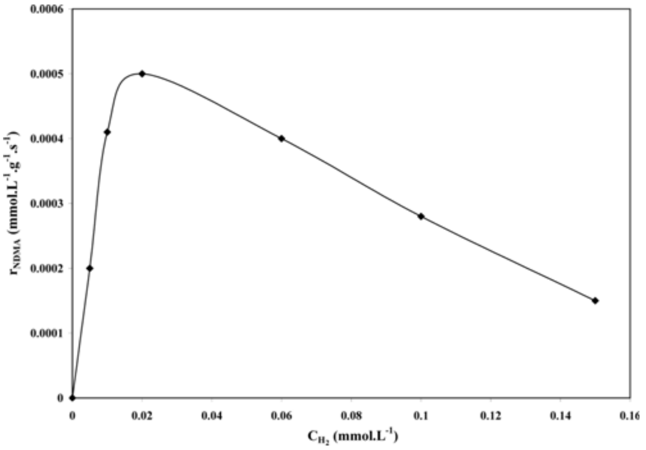

Fig. 7. Reaction rate versus hydrogen concentration at ($C_{o,NDMA}$= 1 mmol·L^{-1}, T=40 °C).

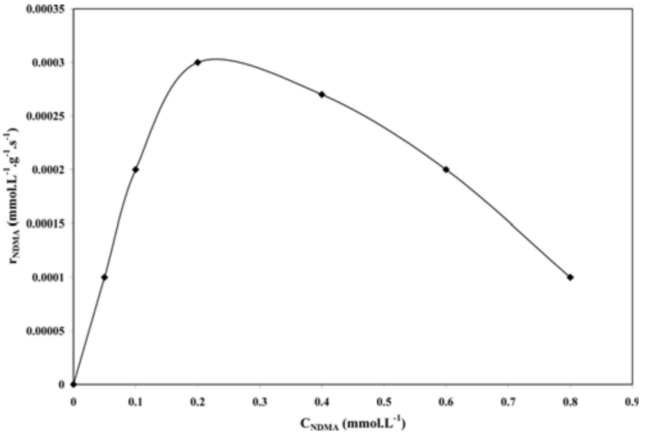

Fig. 8. Reaction rate versus NDMA concentration C_{o,H_2}=1 mmol·L^{-1}, T=40 °C).

After reducing the heat and mass transfer limitations, the kinetic data were obtained for NDMA hydrogenolysis. The reaction rate versus hydrogen and NDMA concentrations are illustrated in Figs. 7 and 8, respectively.

8. Reaction Mechanism

In the presence of Au/γ-Al_2O_3 nanocatalyst, the transformation mechanism of NDMA is postulated to be catalytic hydrogenolysis, resulting in N-N bond breakdown to form DMA and HNO as final products.

H_2 is dissociated on nanosized gold producing atomic hydrogen, which is very reactive and mobile at the metal surface. It may react with adsorbed NDMA. In such reactions the hydrogen molecules are adsorbed and dissociated on the corners and the edges of Au particles [25]. The N-N bond is cleaved or hydrogenolyzed, the amine group is reduced to DMA and the nitrosyl to HNO. Langmuir-Hinshelwood, as a simple mechanism, may explain the reaction steps:

$$H_2+2^* \xleftrightarrow{K_1} 2H^* \tag{5}$$

$$(CH_3)_2NNO+^* \xleftrightarrow{K_2} (CH_3)_2NNO^* \tag{6}$$

$$(CH_3)_2NNO^*+H^* \xleftrightarrow{K_3} (CH_3)_2NNOH^*+^* \tag{7}$$

$$(CH_3)_2NNOH^*+H^* \xleftrightarrow{K_4} (CH_3)_2NHNOH^*+^* \tag{8}$$

$$(CH_3)_2NHNOH^*+^* \xleftrightarrow{K_5} (CH_3)_2NH^*+NOH^* \tag{9}$$

$$(CH_3)_2NH^* \xleftrightarrow{K_6} (CH_3)_2NH+^* \tag{10}$$

$$NOH^* \xleftrightarrow{K_7} HNO+^* \tag{11}$$

where, * represents a surface site and $K_i=(k_i/k_{-i})$ (k_i and k_{-i} are the forward and backward reaction rate constants, respectively).

As mentioned, H_2 is adsorbed and dissociated on gold nanoparticles. The weak adsorption of H_2 on gold nanoparticles has been reported [16].

A reaction between the amine and the metallic surface (Au surface) leads to the formation of organo-metallic complexes; in particular, a monolayer on the Au surface [26].

Dissociated hydrogen is active on the catalyst surface; therefore, it reacts with other adsorbed species [26]. So, k_3>>>k_{-3} and k_4>>>k_{-4}.

The experimental observations showed that there is a good carbon balance between the input NDMA and the output DMA, to a point that the NDMA has no retention on the catalyst surface and desorbs from the surface. Consequently, k_6>>>k_{-6}.

According to classic chemistry, the electrophilic property of oxygen in NOH leads to NOH* which is desorbed quickly from the catalyst surface; hence, k_7>>>k_{-7}. Here, it is assumed that Eq. (9) is the limiting step.

On the basis of the suggested mechanism, the reaction rate is given in the following equation:

$$r_{NDMA}=\frac{k_5K_1K_2C_{H_2}C_{NDMA}}{(1+K_1C_{H_2}+K_2C_{NDMA})^2}=\frac{kK_{H_2}K_{NDMA}C_{H_2}C_{NDMA}}{(1+K_{H_2}C_{H_2}+K_{NDMA}C_{NDMA})^2} \tag{12}$$

According to Fig. 7, at low concentrations of H_2, the reaction rate versus concentration is linear or first order with respect to H_2 concentration. The profile has a maximum rate and then the reaction rate tends to be zero at high concentrations. This behavior is explained through Eq. (12). This is true for NDMA concentration as well.

To find the temperature dependence of k, K_{H_2} and K_{NDMA}, the experiments were carried out with rough equal concentrations of hydrogen and NDMA at temperatures of 10, 20, 30 and 40 °C. MATLAB 7.0 software was used in calculating k, K_{H_2} and K_{NDMA} at these temperatures. lnk versus 1/T is drawn in Fig. 9. Adopting the Arrhenius law, the activation energy for the reaction was calculated as 21.3 kJ/mol. This amount (greater than 20 kJ/mol) confirms that inter-

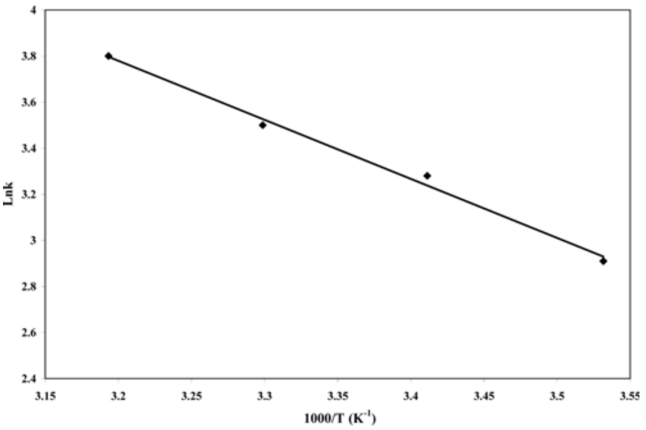

Fig. 9. Dependency of kinetic parameter k on temperature.

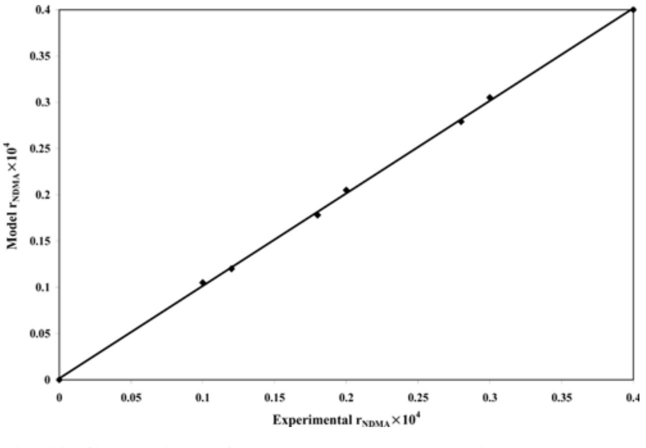

Fig. 10. Comparison of model results and experimental observations for NDMA degradation (T=40 °C, GHSV=20,000 h^{-1}).

phase diffusion limitation is negligible [24], as mentioned before.

The model results (Eq. (12)) agreed well with the experimental observations at T=40 °C and GHSV=20,000 h^{-1}. The comparison between model results and experimental results is illustrated in Fig. 10. Applying Eq. (13), the standard deviation (SD) was ±0.15:

$$SD=\sqrt{\frac{\sum_{i=1}^{N}\frac{(\mathrm{Exp}-\mathrm{Cal})}{\mathrm{Exp}}}{N-1}}=\pm 0.15 \qquad (13)$$

CONCLUSIONS

Due to intriguing properties of Au/γ-Al_2O_3 nanocatalyst, this catalyst was used in reductive destruction of nitrosodimethyl amine (NDMA) in vapor phase. The less toxic and non-carcinogenic products of the reaction were dimethyl amine (DMA) and nitroxyl (HNO). The catalyst was synthesized through the homogeneous deposition-precipitation (HDP)/DP-urea method with trace concentration of chlorine in the samples. The reaction is structure sensitive and exhibits an increase in activity with a decrease in average Au particle size. The proper size for Au particles was <5 nm. The catalyst with loading 1.5 wt% of Au showed suitable activity. The intriguing effect of the catalyst was its performance in low temperatures (10-40 °C). By choosing the parameters and eliminating mass and heat transfer limitations, the reaction kinetic was studied. According to the obtained kinetic data, the Langmuir-Hinshelwood model involving dissociative adsorption of H_2 was proposed. From the model, activation energy was calculated as 21.3 kJ/mol in the temperature range.

NOMENCLATURE

C_{H_2} : H_2 concentration [mmol·L^{-1}]
C_{NDMA} : NDMA concentration [mmol·L^{-1}]
DMA: dimethyl amine $(CH_3)_2NH$
$\bar{d}_p$: average diameter of Au particles [nm]
d_p : catalyst particle diameter [mm]
ID : inner reactor diameter [mm]
k_5 or k : reaction rate constant [mmol·L^{-1}·g^{-1}·s^{-1}]
l : catalyst bed length [cm]
NDMA : nitrosodimethyl amine $(CH_3)_2NNO$
n_i : number of particles of diameter d_i [-]
Q_F : volume rate of feed [mL·min^{-1}]
r_{NDMA} : NDMA reaction rate [mmol·L^{-1}·g^{-1}·s^{-1}]
T : absolute temperature [K]
UDMH : unsymmetrical dimethyl hydrazine $(CH_3)_2NNH_2$
X_{NDMA} : NDMA conversion [-]

Superscript

* : active site of the catalyst

REFERENCES

1. E. W. Schmidt, *Hydrazine and its derivatives (2nd Ed.)*, Wiley, New York (2001).
2. H. Xu, *N-Nitrosamines in the environment*, Science Press, Beijing (1988).
3. B. Xu, Z. Chen, F. Qi, J. Ma and F.Wu, *J. Hazard. Mater.*, **168**, 108 (2009).
4. J. Lee, W. Choi and J. Yon, *Environ. Sci. Technol.*, **39**, 6800 (2005).
5. V. K. Sharma, *Sep. Purif. Technol.*, **88**, 1 (2012).
6. L. Gui, R. W. Gillham and M. S. Odziemkowski, *Environ. Sci. Technol.*, **34**, 3489 (2000).
7. M. G. Davie, M. Reinhard and J. R. Shapley, *Environ. Sci. Technol.*, **40**, 7329 (2006).
8. G. V. Smith and F. Notheisz, *Heterogeneous catalysis in organic chemistry*, Academic Press, New York (1999).
9. M. Haruta, *Catal. Surv. Jpn.*, **1**, 61 (1997).
10. L. L. Santos, P. Serna and A. Corma, *Chem. Eur. J.*, **15**, 8196 (2009).
11. A. Corma and P. Serna, *Science*, **313**, 332 (2006).
12. S. G. Pakdehi and M. Sohrabi, *Chem. Eng. Technol.*, **34**, 1840 (2011).
13. A. Hugon, L. Delannoy, J. M. Krafft and C. Louis, *J. Phys. Chem. C*, **114**, 10823 (2010).
14. S. Shiva, J. H. Crawford, A. Ramachandran, E. K. Ceaser, T. Hillson, P. S. Brookes, R. P. Patel and V. M. Darley-Usmar, *Biochem. J.*, **379**, 359 (2004).
15. V. Shafirovich and S. V. Lymar, *Proceedings of the National Academy of Sciences*, **99**, 7340 (2002).
16. N. N. Greenwood and A. Earnshaw, *Chemistry of the elements*, Elsevier, Oxford (1997).
17. C. Kartusch and J. A. van Bokhoven, *Gold Bull.*, **42**, 343 (2009).
18. G. C. Bond and D. T. Thompson, *Catal. Rev. Sci. Eng.*, **41**, 319 (1999).
19. L. McEwana, M. Juliusa, S. Robertsa and J. C. Q. Fletchera, *Gold Bull.*, **43**, 298 (2010).
20. A. Hussain, *A computational study of catalysis by gold in applications of CO oxidation*, Ph.D. Thesis, Eindhoven: Technische Universiteit Eindhoven (2010).
21. M. Comotti, *Nano-design as a powerful tool in gold catalyzed oxidation reactions*, Ph.D. Thesis, Bochum: Universität Bochum (2007).
22. M. Okumura, T. Akita and M. Haruta, *Catal. Today*, **74**, 265 (2002).
23. D. Huang, F. Liao, S. Molesa, D. Redinger and V. Subramanian, *J. Electrochem. Soc.*, **150**, 412 (2003).
24. C. Perego and S. Peratello, *Catal. Today*, **52**, 133 (1999).
25. T. Ishida, N. Kawakita, T. Akita and M. Haruta, *Gold Bull.*, **42**, 267 (2009).
26. M. Aufray and A. A. Roche, *Appl. Surf. Sci.*, **254**, 1936 (2007).